(4% ether/hexanes) afforded 83 mg (76%) of **10**, mp 102.5–104 °C. Anti Michael adduct **10** was identified by comparison of its ^{1}H NMR spectrum and melting point with those of an authentic sample.[23c]

Reaction with Benzoyl Chloride. To a 10-mL flask in a glovebox was added 106 μL (0.5 mmol) of **3**. The flask was capped with a septum and removed from the glovebox. The septum was pierced with an N_2 inlet needle, and **3** was dissolved in 1 mL of THF. Benzoyl chloride (58 μL, 0.5 mmol, distilled from $CaCO_3$) in 1 mL of THF was added at 0 °C, and after 10 min the reaction mixture was quenched with saturated aqueous $NaHCO_3$. Standard workup afforded a white solid. Chromatography on silica gel using 20:1 hexanes/ethyl acetate as eluant provided 70 mg (65%) of a white solid, mp 89–90.5 °C. Compound **11** was identified by comparison of its ^{1}H NMR spectrum and melting point with those of an authentic sample.[24]

Reaction with Trimethylsilyl Chloride. To a 10-mL flask in a glovebox was added 207 μL (1 mmol) of **3**. Enolate **3** was dissolved in 2 mL of THF, and 152 μL (1.2 mmol) of trimethylsilyl chloride was added. After 15 h, the reaction mixture was diluted with 6 mL of pentane, removed form the glovebox, and partitioned between pentane and saturated aqueous $NaHCO_3$. Standard workup afforded **12** in quantitative crude yield. Bulb-to-bulb distillation (25 °C, 0.05 torr) provided 122 mg (66%) of a colorless oil. Enol silane **12** was identified by comparison of its ^{1}H NMR spectrum with that of an authentic sample.[11,12]

Ethylzinc Diisopropylamide (16). To a 10-mL flask in a glovebox under N_2 was added 253 mg (2.36 mmol) of lithium diisopropylamide.[26] To this solid in 4 mL of ether was added 306 mg (2.36 mmol) of ethylzinc chloride[27] in 3 mL of ether over 2 min. The white suspension was stirred for 15 min and filtered through a fine glass frit. The solvent was removed under vacuum to afford a white foam which was dissolved in 4 mL of pentane and filtered through a fine glass frit to remove some residual lithium chloride. The solvent was removed under vacuum to afford 438 mg (95%) of a gummy, white solid: mp 132–136 °C dec; IR (C_6H_6) 3020–2760, 1465, 1385, 1368, 1160, 910 cm^{-1}; ^{1}H NMR (250 MHz, C_6D_6) δ 0.57 (q, 2, J = 8.1 Hz), 1.08 (d, 12, J = 6.5 Hz), 1.54 (t, 3, J = 8.1 Hz), 3.08 (heptet, 2, J = 6.5 Hz); ^{13}C NMR (125 MHz, C_6D_6) δ 6.246, 13.350, 26.729, 49.468. Anal. Calcd for $C_8H_{19}NZn$: C, 49.37; H, 9.84; N, 7.20. Found: C, 49.44; H, 10.07; N, 7.02.

4-Bromo-2-methyl-2-((trimethylsilyl)oxy)pentan-3-one (21). To a 100-mL flask was added 15 mL of THF and 2.32 mL (16.5 mmol) of diisopropylamine (distilled from CaH_2). The solution was cooled to 0 °C, and 10.5 mL (15.8 mmol) of a 1.5 M solution of n-BuLi in hexane was added via syringe over 5 min. After being stirred 10 min, the solution was cooled to −78 °C and 3.24 mL (15 mmol) of 2-methyl-2-((trimethylsilyl)oxy)pentan-3-one[34] in 15 mL of THF was added over 10 min. After 10 min at −78 °C the reaction mixture was allowed to warm to room temperature. In a separate 100-mL flask, 930 μL (18 mmol) of bromine was added to 15 mL of THF. The solution was cooled to −78 °C, and the enolate solution was added dropwise over 20 min. An additional 10 mL of THF was added during the addition as stirring became slow. The orange bromine color was dissipated when only about half of the enolate solution had been added. The reaction was quenched with 20 mL of saturated aqueous $NaHCO_3$ after 1 min. The mixture was allowed to warm to room temperature and partitioned between pentane and aqueous $NaHSO_3$. The layers were separated, and the aqueous layer was washed with pentane. The combined organic layers were washed sequentially with aqueous $NaHSO_3$ and brine and dried (Na_2SO_4). The solvent was removed with a rotary evaporator to afford 4.39 g of a colorless oil. ^{1}H NMR analysis indicated that the bromo ketone was ca. 90% pure. Distillation at 25 torr caused significant decomposition; however, the pink fractions boiling between 112 and 121 °C were purified by bulb-to-bulb distillation at 0.03 torr to afford 2.58 g (64%) of **21** as a colorless oil. An unidentified impurity (<10%) remained which was not removed by subsequent distillation at 1.2 torr: IR (film) 2970, 1725, 1260, 1205, 1050, 895, 850 cm^{-1}; ^{1}H NMR (250 MHz, $CDCl_3$) δ 0.19 (s, 9), 1.35 (s, 3), 1.54 (s, 3), 1.71 (d, 3, J = 6.8 Hz), 5.18 (q, 1, J = 6.8 Hz); ^{13}C NMR (125 MHz, $CDCl_3$) δ 2.197, 20.709, 27.882, 28.898, 39.848, 79.934, 208.947. An analytical sample was prepared by preparative GC. Anal. Calcd for $C_9H_{19}O_2BrSi$: C, 40.45; H, 7.17; Br, 29.90. Found: C, 40.33; H, 7.28; Br, 29.84.

Acknowledgment. This research was supported by a research grant from the United States Public Health Service (AI 15027). M.M.H. gratefully acknowledges the National Science Foundation for a Predoctoral Fellowship.

Synthesis, Structure, and Ligand Dynamics of $(\mu\text{-H})(\mu_3\text{-}\eta^2\text{-CH}_3\text{C=NCH}_2\text{CH}_3)\text{Ru}_3(\text{CO})_9$

Silvio Aime,* Roberto Gobetto, Franco Padovan, and Mauro Botta

Istituto di Chimica Inorganica, Università di Torino, Turin, Italy

Edward Rosenberg*

Department of Chemistry, California State University, Northridge, California 91330

Robert W. Gellert

Department of Chemistry, California State University, Los Angeles, California

Received January 6, 1987

The reaction of triethylamine with $Ru_3(CO)_{12}$ in refluxing hexanes catalyzed by $Fe_2(CO)_4(SEt)_2(PPh_3)_2$ is shown to yield the complex $(\mu\text{-H})Ru_3(CO)_9(\mu_3\text{-}\eta^2\text{-CH}_3\text{C=NCH}_2\text{CH}_3)$ (I) as the major product (30%). An X-ray crystallographic investigation of I reveals that the organic ligand is parallel to one edge of the metal triangle and acts as a five-electron donor. The hydride was located; it symmetrically bridges the two metal atoms parallel to the C–N vector and is in the plane of the metal triangle. Compound I crystallizes in the $P\bar{1}$ space group with α = 8.396 (2) Å, b = 15.198 (3) Å, c = 8.093 (2) Å, α = 102.95 (2)°, β = 108.63 (2)°, and γ = 90.33 (2)°. Least-squares refinement based on 2867 observed reflections led to a final R value of 3.3% (R_w = 4.4%). The variable-temperature ^{1}H and ^{13}C NMR spectra reveal that the organic ligand is fluxional, undergoing restricted oscillatory motion which is coupled to hydride edge hopping and axial–radial exchange on two of the three ruthenium atoms.

Introduction

The cleavage of nitrogen–carbon bonds by heterogeneous transition-metal catalysts and metal cluster complexes is an area of current interest because of the importance of developing denitrification procedures for coal and petroleum refining processes.[1] Trinuclear clusters of ruthenium

0276-7333/87/2306-2074$01.50/0

Table I. Bond Distances (Å) and Angles (deg) for $HRu_3(CO)_9(CH_3CNCH_2CH_3)$

Bond Distances

Ru(1)–Ru(2)	2.720 (1)	Ru(2)–C(3)	2.263 (6)	C(21)–O(21)	1.136 (10)
Ru(1)–Ru(3)	2.92 (1)	Ru(2)–N(4)	2.222 (5)	C(22)–O(22)	1.136 (10)
Ru(2)–Ru(3)	2.696 (1)	Ru(3)–H	1.80	C(23)–O(23)	1.125 (10)
Ru(1)–H	1.76	Ru(3)–C(31)	1.942 (7)	C(31)–O(31)	1.124 (10)
Ru(1)–C(11)	1.904 (7)	Ru(3)–C(32)	1.934 (7)	C(32)–O(32)	1.117 (9)
Ru(1)–C(12)	1.891 (7)	Ru(3)–C(33)	1.904 (7)	C(33)–O(33)	1.129 (9)
Ru(1)–C(13)	1.947 (7)	Ru(3)–N(4)	2.086 (5)	C(1)–C(22)	1.363 (27)
Ru(1)–C(3)	2.081 (5)	C(11)–O(11)	1.149 (10)	C(2)–C(3)	1.515 (9)
Ru(2)–C(21)	1.911 (7)	C(11)–O(11)	1.149 (10)	C(3)–N(4)	1.343 (8)
Ru(2)–C(22)	1.869 (8)	C(12)–O(12)	1.148 (9)	N(4)–C(5)	1.503 (9)
Ru(2)–C(23)	1.915 (8)	C(13)–O(13)	1.129 (9)	C(5)–C(6)	1.445 (14)

Bond Angles

Ru(2)–Ru(1)–Ru(3)	56.92 (2)	C(21)–Ru(2)–C(23)	95.7 (3)	Ru(1)–C(11)–O(11)	178.7 (7)
C(12)–Ru(1)–C(11)	96.5 (3)	C(21)–Ru(2)–Ru(3)	97.8 (2)	Ru(1)–C(12)–O(12)	178.6 (7)
C(12)–Ru(1)–C(13)	91.3 (3)	C(21)–Ru(2)–Ru(1)	162.6 (2)	Ru(1)–C(13)–O(13)	178.4 (6)
C(12)–Ru(1)–Ru(2)	94.0 (2)	C(23)–Ru(2)–Ru(3)	163.1 (3)	Ru(2)–C(21)–O(21)	178.6 (7)
C(12)–Ru(1)–Ru(3)	150.5 (2)	C(23)–Ru(2)–Ru(1)	100.1 (2)	Ru(2)–C(22)–O(22)	177.7 (7)
C(11)–Ru(1)–C(13)	99.2 (3)	Ru(2)–Ru(3)–Ru(1)	57.70 (2)	Ru(2)–C(23)–O(23)	178.8 (8)
C(11)–Ru(1)–Ru(2)	154.2 (2)	C(33)–Ru(3)–C(32)	91.2 (3)	Ru(3)–C(31)–O(31)	178.8 (7)
C(11)–Ru(1)–Ru(3)	108.5 (2)	C(33)–Ru(3)–C(31)	96.7 (3)	Ru(3)–C(32)–O(32)	177.7 (6)
C(13)–Ru(1)–Ru(2)	104.1 (2)	C(33)–Ru(3)–Ru(2)	94.6 (2)	Ru(3)–C(33)–O(33)	178.4 (6)
C(13)–Ru(1)–Ru(3)	99.7 (2)	C(33)–Ru(3)–Ru(1)	152.0 (2)	C(1)–C(2)–C(3)	111.3 (10)
H–Ru(1)–C(12)	174	C(32)–Ru(3)–C(31)	97.1 (3)	N(4)–C(3)–C(2)	121.5 (5)
H–Ru(1)–C(11)	77.0	C(32)–Ru(3)–Ru(2)	104.4 (2)	C(2)–C(3)–Ru(1)	125.7 (4)
H–Ru(1)–C(13)	90.0	C(32)–Ru(3)–Ru(1)	99.1 (2)	N(4–)C(3)–Ru(1)	112.4 (4)
H–Ru(1)–Ru(2)	92.0	C(31)–Ru(3)–Ru(2)	155.5 (2)	Ru(1)–C(3)–Ru(2)	77.4 (2)
H–Ru(1)–Ru(3)	35.2	C(31)–Ru(3)–Ru(1)	107.6 (2)	C(3)–N(4)–C(5)	121.8 (5)
Ru(3)–Ru(2)–Ru(1)	65.4 (2)	H–Ru(3)–C(33)	173.0	C(3)–N(4)–Ru(3)	112.1 (4)
C(22)–Ru(2)–C(21)	97.0 (3)	H–Ru(3)–C(32)	89.1	Ru(3)–N(4)–C(5)	125.4 (4)
C(22)–Ru(2)–C(23)	96.4 (3)	H–Ru(3)–C(31)	76.5	Ru(2)–N(4)–Ru(3)	77.4 (2)
C(22)–Ru(2)–Ru(3)	92.0 (2)	H–Ru(3)–Ru(2)	92.0	C(6)–C(5)–N(4)	110.9 (6)
C(22)–Ru(2)–Ru(1)	88.4 (2)	H–Ru(3)–Ru(1)	34.3		

and osmium have been shown to be effective transalkylation catalysts for mixtures of tertiary amines,[2] and a preliminary report on the isolation of a possible intermediate in the nitrogen–carbon bond cleaving process $(\mu\text{-}H)(\mu_3\text{-}\eta^2\text{-}CH_3CH_2N{=}CCH_3)Ru_3(CO)_9$ (I) has appeared.[3] We recently discovered that binuclear complexes which readily form mononuclear radicals at low temperatures (<70 °C) can affect ligand substitution of carbon monoxide in ruthenium carbonyls, presumably by promoting metal–metal bond cleavage at temperatures well below those required for rapid carbonyl dissociation.[4] It occurred to us that with use of these binuclear catalysts we might be able to promote the reaction of tertiary amines with ruthenium carbonyls directly at the metal leading to amine complexes which could then undergo the facile carbon–nitrogen bond cleavage processes suggested to occur catalytically, in a stoichiometric sense. We report here the results of a study in which the reaction of triethylamine with ruthenium carbonyl catalyzed by $Fe_2(CO)_4(\mu\text{-}SEt)_2(PPh_3)_2$ is shown to give I in sufficient yield for complete characterization. In addition we have isolated a family of triruthenium–triethylamine derivatives that appear to be precursors to I. The complete characterization of these products is not possible at this time due to their low yield, and we report here the solid-state structure and solution ligand dynamics of the major product I.

Results and Discussion

The reaction of ruthenium carbonyl with excess triethylamine in refluxing hexanes in the presence of a catalytic amount of $Fe_2(CO)_4(\mu\text{-}SEt)_2(PPh_3)_2$ for 6 h gives four product bands in addition to a small amount of unreacted ruthenium carbonyl on purification by preparative thin-layer chromatography on silica gel. We have completely characterized the third band I which is obtained in about a 30% yield; a significant improvement over the previously reported synthesis which did not employ a metal radical promoter.[3] Characterization of the other products is currently underway utilizing lower boiling solvents and greater concentrations of catalyst.

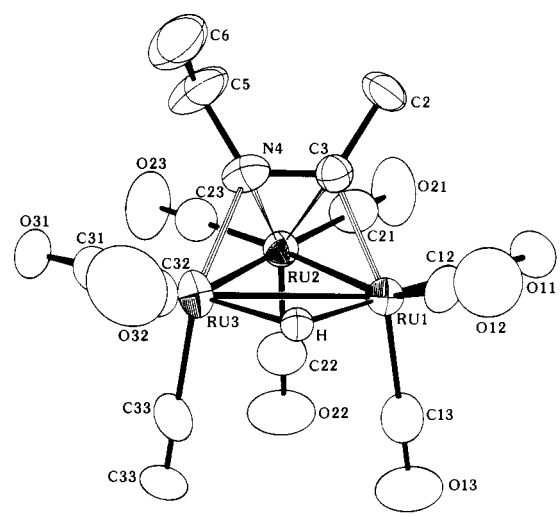

Figure 1. Solid-state structure of $(\mu\text{-}H)(\mu_3\text{-}\eta^2\text{-}CH_3C{=}NCH_2CH_3)Ru_3(CO)_9$ (I).

(A) Solid-State Structure of I. The solid-state structure of I is shown in Figure 1. All ligand atoms including the hydride hydrogen were located, and a table of selected bond distances and angles is given in Table I. The structure consists of an approximate isosceles triangle of metal atoms with the long edge (Ru(1)–Ru(3) = 2.925

(1) Satterfield, C. N.; Gultekin, S. *Ind. Eng. Chem. Proc. Des. Dev.* **1981**, *20*, 62.
(2) Laine, R. M.; Thomas, D. W.; Cary, L. W. *J. Am. Chem. Soc.* **1982**, *104*, 1763.
(3) Laine, R. M. *Ann. New York Acad. Sci.* **1985**, 271.
(4) Aime, S.; Botta, M.; Gobetto R.; Osella, D. *Organometallics* **1985**, *4*, 1475.

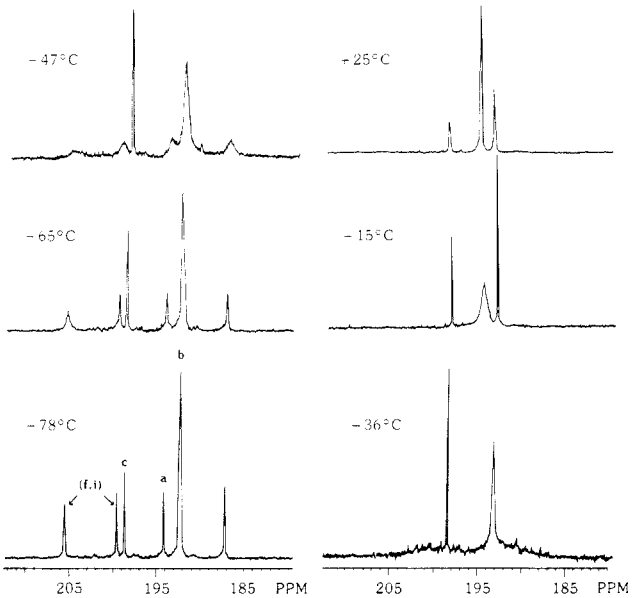

Figure 2. Variable-temperature ^{13}C NMR of I at 67.8 MHz in toluene-d_8.

(2) Å) having the hydride bridge. The hydride ligand is located in the plane of the Ru_3 triangle and is symmetrically disposed between Ru(1) and Ru(3). The hydride is approximately trans to one of the two equatorial carbonyls (H–Ru–C(12) = 174.0 (2)°). The locations of the nine carbonyl groups are standard with respect to the many $Ru_3(CO)_9$ structures previously reported, there being three axial and six equatorial groups. The organic ligand in I consists of μ_3-η^2-imine. The ligand is essentially parallel to the Ru(1)–Ru(3) edge with the Ru(1)–C(3) distance of 2.081 (5) Å being almost equal to the Ru(3)–N(4) distance of 2.086 (5) Å and the Ru(2)–N(4) and Ru(2)–C(3) distances being 2.222 (5) and 2.263 (6) Å, respectively. The C(3)–N(4) distance of 1.343 (8) Å and the N(4)–C(3)–C(2) and C(3)–N(4)–C(5) bond angles of 121.5 (5)° clearly indicate the presence of a carbon–nitrogen double bond and sp^2 hybridization at the metal-bound ligand atoms. The organic ligand thus must act as a five-electron donor making I a saturated 48e cluster when one includes the hydride and the nine carbonyl groups. This structure is virtually identical with the triosmium clusters reported by Adams (μ-H)(μ_3-η^2-HC=NC_6H_5)$Os_3(CO)_9$[5a] and the ruthenium complex (μ-H)$Ru_3(CO)_{10}$(μ_3-η^2-$C_{13}H_{18}N$)[5b] in terms of the disposition of the organic ligand on the trinuclear cluster.

(B) Variable-Temperature ^{13}C and ^1H NMR of I. The room-temperature ^{13}C NMR of I in toluene-d_8 shows three resonances at 198.1, 194.6, and 193.1 ppm in a ratio of 1:6:2 (Figure 2). Since this complex has no symmetry elements, nine separate resonances should be observed and so it seemed likely that some dynamic process is operative at room temperature. We therefore examined the variable-temperature ^{13}C NMR of I in toluene-d_8. The low-temperature limiting spectrum is realized at −28 °C where six resonances are observed at 205.6, 199.6, 198.6, 194.2, 192.3, and 187.2 ppm in a relative intensity ratio of 1:1:1:1:4:1. When the proton decoupler is off, the peak at 194.2 ppm splits into a doublet (^2J(C–H) = 9.0 Hz) and the peak of relative intensity four at 192.3 ppm splits into a doublet of unequal intensity, indicating that this resonances is actually a set of overlapping resonances, one of

Scheme I

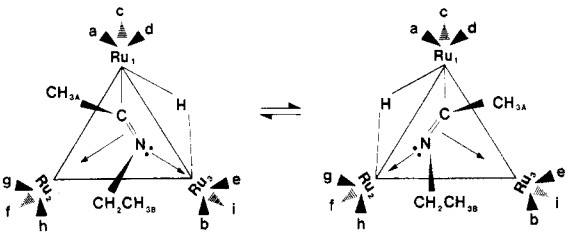

which is coupled to the hydride. We therefore assign the resonance at 194.2 ppm and one of the overlapping resonances at 192.3 ppm to the two equatorial carbonyl groups trans to the hydride on Ru(1) and Ru(3).[6] As the temperature is increased to −65 °C, all the resonances broaden except the one at 198.6 ppm; at −47 °C, a new broad resonance appears which is the weighted average of the hydride-coupled resonance at 194.2 ppm and one of the overlapping resonances at 192.3 ppm. At −36 °C this resonance continues to sharpen, the resonance at 198.6 ppm remains sharp, and the remaining resonances (total relative intensity = 6) are all broadened into the base line. These six resonances emerge as a single resonance at 194.6 ppm at −150 °C which is the weighted average of the resonances at 205.6, 199.6, and 187.2 ppm and the three remaining overlapping resonances at 192.3 ppm. The operative dynamic processes thus averages two resonances with each other and simultaneously averages six resonances leaving one unchanged. Although we cannot completely assign all the resonances based on this information, partial assignments can be made with an understanding of the observed dynamic processes. An oscillatory motion of the organic ligand pivoting on the carbon atom only and coupled with axial–radial exchange at Ru(2) and Ru(3) and edge hopping of the hydride ligand readily explains the observed spectral changes (Scheme I). With this dynamic process in mind (and the ^2J(C–H) coupling) we can assign the resonance at 194.2 ppm to carbonyl a and one of the overlapping resonances at 192.3 ppm to carbonyl b (see Scheme I). The resonances at 205.6 and 199.6 ppm can be assigned interchangably to the axial carbonyls f and i on the basis of their downfield chemical shift and dynamic behavior. The resonance at 198.6 ppm is similarly assigned to the axial carbonyl c and the remaining resonance at 187.2 ppm of relative intensity one, and the remaining ones at 192.3 ppm are interchangably assigned to the remaining four equatorial carbonyls d, e, h and g.

The variable-temperature ^1H NMR of I is entirely consistent with the dynamic processes outlined above. At −78 °C a slightly broadened AMX_3 pattern is observed which coalesces to a normal ethyl group pattern at room temperature (Figure 3). An estimate of the free energy of activation for this process can be made from the ^1H NMR data with a coalescence temperature of −65 °C. The calculated value of 41.92 kJ/mol (±2 kJ/mol) is in excellent agreement with the value estimated from the coalescence of carbonyl groups a and b (Scheme I) which is 42.33 kJ/mol with a coalescence temperature of −56 °C. This clearly shows that the oscillatory motion of the organic ligand and the edge hopping of the hydride is directly coupled to the observed averaging of the carbonyl groups. Of course we cannot rigorously exclude the possibility that the observed restricted motion of the organic pivots around the nitrogen atom instead of the carbon atom. It seems reasonable, however, that migration of the 2e donor N⇒Ru bond would be a lower energy process than migration of

(5) (a) Adams, R. D. *Acc. Chem. Res.* **1983**, *16*, 67. (b) Fish, R. H.; Kim, J. J.; Stewart, J. L.; Bushweller, J. H.; Rosen, R. K.; Dupon, J. W. *Organometallics* **1986**, *5*, 2193.

(6) Milone, L.; Aime, S. *Prog. Nucl. Magn. Reson.* **1978**, *11*, 183.

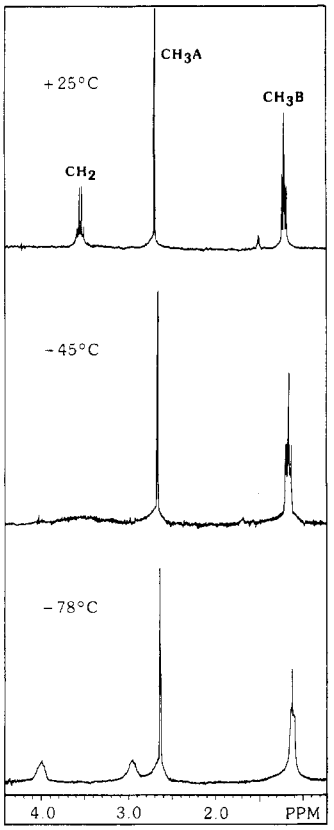

Figure 3. Variable-temperature ^1H NMR of I at 270 MHz in CD_2Cl_2.

the carbon atom which would formally require a homolytic or heterolytic bond cleavage. In fact a directly analogous restricted ligand motion is observed for the σ-π-allenic complex $(\mu\text{-}H)(\mu_3\text{-}\eta^3\text{-}CH_3C{=}C{=}C(CH_3)CH_3)Ru_3(CO)_9$ in which the π-bonds oscillate between two atoms coupled with edge hopping of the hydride and axial–radial exchange at the π-coordinated Ru atoms.[7] In the case of the allenic system there is no ambiguity as to which end of the organic ligand is migrating and dissociation of the 2e bond is clearly a lower energy process than migration of the σ-Ru–C bond. The dynamic process observed for I has an even lower activation energy than the analogous process in the allenic complex. Indeed the observed free energy of activation is the lowest reported to date for any 5e donor bound to an Ru_3 face.[8] Further studies on the reactivity of I and an extension of the synthesis of I to other amines are underway in order to further elucidate the reasons for and consequences of the high degree of mobility of the organic ligand in I.

Experimental Materials

$Ru_3(CO)_{12}$ was purchased from Strem Chemicals. Triethylamine and ethanethiol were purchased from Carlo Erba and used as received. The catalyst $Fe_2(CO)_4(\mu\text{-}SEt)_2(PPh_3)_2$ was synthesized according to published literature procedures using $Fe_3(CO)_{12}$ and triphenylphosine purchased from Strem Chemicals.[4] Hexane and cyclohexane from Carlo Erba were dried over molecular sieves (4 Å). Deuteriated NMR solvents (toluene-d^8, CD_2Cl_2) were purchased from Aldrich.

Spectra. ^1H and ^{13}C NMR were obtained on a JEOL GX270 spectrometer at 270 and 67.8 MHz, respectively. Temperature measurements were calibrated against a sample of methanol by using the $HOCH_3$ (Δ, ppm). Estimates of the free energy of activation were obtained by using standard equations.[9] Infrared spectra were run in cyclohexane and obtained on a Perkin-Elmer 580B spectrometer.

Table II. Crystal Data: Collection and Refinement Parameters

formula	$HRu_3(CO)_9(\mu_3\text{-}\eta^2\text{-}CH_3CNCH_2CH_3)$
fw	626.4
cryst system, space group	triclinic, $P\bar{1}$
a, Å	8.397 (2)
b, Å	15.205 (3)
c, Å	8.091 (2)
α, deg	102.94 (2)
β, deg	108.66 (2)
γ, deg	90.32 (2)
V, Å^3	950.5 (4)
Z	2
d_{calcd}, g/cm^3	2.189
abs coeff, μ (cm^{-1})	23.51
data collctn temp, °C	23 (±2)
radiation (λ, Å)	Mo K_α (0.710 69)
monochromator	graphite
scan mode	ω–2θ
scan limits, deg	$2.5 < 2\theta \leq 50$
scan speed, deg/min	variable, 1.75–29.3
scan range, deg	1.0
bkgd, deg above K_{α_1}/below K_{α_2}	1.0/1.0
ratio bkgd/scan time	0.5
std reflctns	($\bar{1}$61); (300); (301)
no. of data collcd	3471 ($\pm h,+k,\pm l$)
no. of observns [$F_o^2 > 3\sigma(F_o^2)$]	2867
no. of variables	244
R^a (R all)	0.033 (0.043)
$R_w{}^b$ (R_w all)	0.044 (0.046)
GOF^c	1.60

$^aR = \sum(|F_o| - |F_c|)/\sum|F_o|$. $^bR_w = [\sum w(|F_o| - |F_c|)^2/\sum w|F_o|^2]^{1/2}$. ^{c}GOF $= [\sum w(|F_o| - |F_c|)^2/(N_{observns} - N_{parameters})]^{1/2}$

Synthesis of $Ru_3(\mu\text{-}H)(\mu_3\text{-}\eta^2\text{-}CH_3C{=}NCH_2cH_3)(CO)_9$ (I). $Ru_3(CO)_{12}$ (300 mg, 0.45 mmol), $Fe_2(CO)_4(SEt)_2(PPh_3)_2$ (20 mg, 0.025 mmol), triethylamine (2.0 mL, 14.0 mmol), and hexanes (150 mL) were combined in a round-bottom flask and solvent degassed with nitrogen. The reaction mixture was refluxed under nitrogen atmosphere for 6 h. The red solution was filtered, rotary evaporated, taken up in 2–5 mL of methylene chloride, and purified by preparative thin-layer chromatography using 30–60 petroleum ether as eluent. Six bands eluted in addition to a red band which was identified as the iron dimer catalyst. The top band is unreacted $Ru_3(CO)_{12}$. The third and major yellow band was extracted with methylene chloride and crystallized from hexane to yield 90 mg (30%) of $Ru_3(\mu\text{-}H)(\mu_3\text{-}\eta^2\text{-}CH_3C{=}NCH_2CH_3)(CO)_9$. Anal. Calcd: C, 24.92; H, 1.43. Found: C, 24.87; H, 1.51. Infrared (cyclohexane): ν(CO) 2091 (m), 2064 (s), 2036 (vs), 2020 (s), 2007 (m), 2002 (m), 1996 (m), 1977 (br) cm^{-1}.

Yellow bands two and five (40 mg, ~15% each) and yellow band six (40 mg, ~15%) all appear to contain mixtures of similar compounds or isomers. Their infrared and ^1H NMR spectra suggest that they are triruthenium derivatives, but none of these bands have been sufficiently purified to permit identification of compounds therein.

X-ray Structure Determination of $HRu_3(CO)_9(MeC{=}NEt)$. Single crystals of this compound were obtained by cooling a saturated hexane solution to −20 °C. X-ray data were collected on a light yellow diamond-shaped crystal (0.40 × 0.39 × 0.25 mm^3) by using a four-circle Nicolet (Syntex) $P2_1$ diffractometer and monochromatic Mo Kα radiation. Accurate unit cell dimensions and orientation matrix were obtained from least-squares treatment of 15 high-angle reflections in the range $28° < 2\theta < 34°$. Axial photographs indicated no higher symmetry than triclinic. Details of the data collection parameters and crystal data are given in Table II. Data reduction (which included Lorentz, polarization, and absorption[10] corrections) were performed with the local

(7) Rosenberg, E.; Aime, S.; Milone, L.; Gobetto, R. *Organometallics* **1982**, *1*, 640.
(8) Aime, S.; Osella, D.; Gobetto, R.; Grannozi, G. *Inorg. Chem.* **1986**, *25*, 4004.
(9) Jackman, L. M.; Cotton, F. A. *Dynamic NMR Spectroscopy*; Academic: New York, 1975.

Table III. Positional Parameters and Their Estimated Standard Deviations for $HRu_3(CO)_9(EtN{=}CMe)$[a]

atom	x	y	z	B, Å²
Ru(1)	0.22033 (6)	0.83253 (3)	0.37496 (6)	3.14 (1)
Ru(2)	0.13575 (6)	0.76799 (3)	0.62596 (6)	3.22 (1)
Ru(3)	0.22053 (6)	0.64117 (3)	0.38402 (6)	3.06 (1)
C(11)	0.3696 (8)	0.8559 (5)	0.2524 (9)	4.53 (20)
O(11)	0.4603 (7)	0.8684 (4)	0.1781 (8)	7.35 (21)
C(12)	0.2052 (9)	0.9550 (5)	0.4815 (10)	4.90 (21)
O(12)	0.1924 (8)	1.0289 (3)	0.5452 (9)	7.82 (22)
C(13)	0.0061 (9)	0.8293 (4)	0.1856 (9)	4.58 (20)
O(13)	−0.1179 (7)	0.8254 (4)	0.0743 (8)	7.12 (20)
C(21)	0.1087 (9)	0.6918 (5)	0.7753 (9)	4.72 (21)
O(21)	0.0897 (9)	0.6456 (4)	0.8612 (8)	8.25 (24)
C(22)	−0.0894 (9)	0.7559 (5)	0.4781 (9)	5.04 (22)
O(22)	−0.2265 (7)	0.7455 (5)	0.3880 (8)	7.48 (22)
C(23)	0.1236 (10)	0.8796 (5)	0.7859 (9)	5.38 (23)
O(23)	0.1135 (10)	0.9450 (4)	0.8786 (8)	8.91 (26)
C(31)	0.3672 (9)	0.5853 (4)	0.2547 (9)	4.53 (20)
O(31)	0.4543 (7)	0.5540 (4)	0.1818 (9)	7.91 (22)
C(32)	0.0087 (8)	0.5964 (4)	0.1955 (9)	4.04 (18)
O(32)	−0.1162 (6)	0.5726 (4)	0.0893 (7)	5.79 (16)
C(33)	0.2046 (8)	0.5453 (4)	0.4958 (9)	4.40 (20)
O(33)	0.1919 (7)	0.4876 (4)	0.5588 (8)	7.16 (20)
C(1)	0.6624 (30)	0.8887 (14)	0.7195 (26)	5.67 (69)
C(2)	0.5159 (8)	0.8827 (5)	0.7565 (9)	4.78 (21)
C(3)	0.3885 (7)	0.8117 (4)	0.6123 (7)	2.96 (14)
N(4)	0.3860 (6)	0.7242 (3)	0.6189 (6)	3.51 (13)
C(5)	0.5099 (8)	0.6916 (5)	0.7683 (9)	4.89 (21)
C(6)	0.6607 (13)	0.6674 (8)	0.7254 (14)	5.24 (34)

[a] Anisotropically refined atoms are given in the form of the isotropic equivalent thermal parameter defines as $(^4/_3)[a^2B_{11} + b^2B_{22} + c^2B_{33} + ab(\cos\gamma)B_{12} + ac(\cos\beta)B_{13} + bc(\cos\alpha)B_{23}]$.

program PROCESS. The intensities of three selected standards were measured every 50 reflections to test for instrumental and crystal stability. No significant variation was observed over the course of data collection. Neutral atomic scattering factors were used for all non-hydrogen atoms, and anomalous dispersion[11] corrections for Ru were included in the structure factor calculation.

The crystal structure was solved in the centrosymmetric space group $P\bar{1}$ by the combined Patterson and direct methods (MULTAN)[12] which yielded the coordinates of the three ruthenium atoms. The positions of the remaining non-hydrogen atoms were located from successive structure factor and difference Fourier syntheses. A packing disorder in the crystal gave rise to the presence of a two-carbon fragment in the electron density map at both ends of the imino ligand. The terminal carbon atoms (C(1) and C(6)) of the disordered ethyl group were assigned an occupancy factor of 0.5 in the initial stages of refinement. Site occupancies of the nitrogen, N(4), and carbon, C(3) atoms through which the imino group is bonded to the triruthenium framework were not resolved during subsequent refinement. The structure was refined by full-matrix least squares[13] with isotropic thermal parameters for O, C, and N atoms while ruthenium atoms were treated anisotropically. At this stage of refinement the occupancy factors of the terminal ethyl carbon atom were varied. The relative populations of this atom converged, after three cycles of refinement, to 0.35 for C(1) and 0.65 for C(6). In the last stages of refinement anisotropic temperature factors were employed for all non-hydrogen atoms with fixed occupancy factors for the terminal ethyl carbon atom. The function minimized during refinement was $\sum w(|F_o| - F_c|)^2$ with $w = 1/\sigma^2(F_o)$.[14] While a final difference electron density map showed only three of the eight hydrogen atoms of the imino ligand at reasonable positions, it clearly revealed a positive residual density at the expected position of the hydrido hydrogen (Ru(1)–H–Ru(3)) (Figure 1).

Acknowledgment. We gratefully acknowledge the National Science Foundation (Grant CHE8712047), the donors to Petroleum Research Fund, administered by the American Chemical Society, and the CNR of Italy for a Nato Fellowship.

Registry No. I, 91593-44-1; $Fe_2(CO)_4(SEt)_2(PPh_3)_2$, 108241-51-6; $Ru_3(CO)_{12}$, 15243-33-1; triethylamine, 121-44-8.

Supplementary Material Available: A table of anisotropic thermal parameters (1 page); a complete listing of the observed and calculated structure factor amplitudes (16 pages). Ordering information is given on any current masthead page.

(10) An empirical absorption correction was performed by using the ψ-scan technique, which is based on the variation of the intensity of a selected reflection (161) about the ψ-axis.

(11) Atomic scattering factors and anomalous dispersion corrections were taken from the following sources: Cromer, D. T.; Waber, J. T. *International Tables for X-Ray Crystallography*; Kynock: Birmingham England, 1974; Vol. IV, Table 2.2A. Cromer, D. T. *Ibid., Table* 2.3.1.

(12) MULTAN: A system of computer programs for the automatic solution of crystal structures from X-ray diffraction data: Germain, G.; Main, P.; Woolfson, M. M. *Acta Crystallogr., Sect. A: Cryst. Phys., Diffr., Theor. Gen. Crystallogr.* **1971**, *A27*, 368.

(13) CRYGLS, a locally modified version of ORFLS, full-matrix least squares by W. R. Busing and H. A. Levy. All computational work was performed on the CDC-Cyber 170–760 at the State University Data Center and CSULA.

(14) $R_F = \sum(|F_o| - |F_c|)/\sum F_o$, $R_{wF} = [\sum w(|F_o| - |F_c|)^2/\sum wF_o^2]^{1/2}$, $w = 4F_o^2/(\sigma^2(F_o^2) + (pF_o^2)^2)$, with $p = 0.04$ and $\sigma(R_o^2)$ based on counting statistics alone, and GOF $= [\sum w(|F_o| - |F_c|^2/(N_o - N_v)]^{1/2}$, where $N_o = 2867$ and $N_v = 244$ are the number of observations and the number of variables, respectively.